HHS Public Access

Author manuscript

Sci Signal. Author manuscript; available in PMC 2020 February 03.

Published in final edited form as:

Sci Signal. ; 12(597): . doi:10.1126/scisignal.aax3332.

Diacylglycerol kinase ζ promotes allergic airway inflammation and airway hyperresponsiveness through distinct mechanisms

Brenal K. Singh[1,*], **Wen Lu**[1,*], **Amanda M. Schmidt Paustian**[1], **Moyar Q. Ge**[2], **Cynthia J. Koziol-White**[3], **Cameron H. Flayer**[2], **Sara S. Killingbeck**[2], **Nadan Wang**[4], **Xinzhong Dong**[5], **Matthew J. Riese**[6], **Deepak A. Deshpande**[4], **Reynold A. Panettieri Jr.**[3], **Angela Haczku**[2], **Taku Kambayashi**[1,*,†]

[1]Department of Pathology and Laboratory Medicine, Perelman School of Medicine at the University of Pennsylvania, Philadelphia, PA 19104, USA.

[2]Pulmonary, Critical Care and Sleep Division, University of California, Davis, Davis, CA 95616, USA.

[3]Rutgers Institute for Translational Medicine and Science, Rutgers University, New Brunswick, NJ 08901, USA.

[4]Department of Medicine, Center for Translational Medicine, Thomas Jefferson University, Philadelphia, PA 19107, USA.

[5]The Solomon H. Snyder Department of Neuroscience, Center for Sensory Biology, School of Medicine, Johns Hopkins University, Baltimore, MD 21205, USA.

[6]Blood Research Institute, Blood Center of Wisconsin, Milwaukee, WI 53226, USA.

Abstract

Asthma is a chronic allergic inflammatory airway disease caused by aberrant immune responses to inhaled allergens, which leads to airway hyperresponsiveness (AHR) to contractile stimuli and airway obstruction. Blocking T helper 2 (T_H2) differentiation represents a viable therapeutic strategy for allergic asthma, and strong TCR-mediated ERK activation blocks T_H2 differentiation. Here, we report that targeting diacylglycerol (DAG) kinase zeta (DGKζ), a negative regulator of DAG-mediated cell signaling, protected against allergic asthma by simultaneously reducing airway inflammation and AHR though independent mechanisms. Targeted deletion of DGKζ in T cells decreased type 2 inflammation without reducing AHR. In contrast, loss of DGKζ in airway smooth muscle cells decreased AHR but not airway inflammation. T cell–specific enhancement of

[†]Corresponding author. kambayat@pennmedicine.upenn.edu.
[*]These authors contributed equally to this work.

Author contributions: B.K.S., W.L., A.M.S.P., A.H., R.A.P., D.A.D., and T.K. designed the experiments. B.K.S., W.L., A.M.S.P., M.Q.G., N.W., C.J.K.-W., and T.K. performed the experiments. C.H.F. and S.S.K. scored the histopathological specimens. M.J.R. and X.D. provided valuable reagents. T.K. conceived and supervised the project. The manuscript was written by B.K.S. and T.K. and edited by all authors.

Competing interests: The authors declare that they have no competing financial interests.

Data and materials availability: All data needed to evaluate the conclusions in the paper are present in the paper or the Supplementary Materials.

SUPPLEMENTARY MATERIALS
stke.sciencemag.org/cgi/content/full/12/597/eaax3332/DC1

ERK signaling was only sufficient to limit type 2 airway inflammation, not AHR. Pharmacological inhibition of DGK diminished both airway inflammation and AHR in mice and also reduced bronchoconstriction of human airway samples in vitro. These data suggest that DGK is a previously unrecognized therapeutic target for asthma and reveal that the inflammatory and AHR components of asthma are not as interdependent as generally believed.

INTRODUCTION

Asthma is a chronic allergic inflammatory airway disease that affects more than 300 million people worldwide, with an annual economic cost estimated to exceed $56 billion in the United States alone (1). The pathogenesis associated with allergic asthma is characterized by airway inflammation that is mediated by aberrant immune responses to inhaled allergens at the mucosal surfaces of the lung and airflow obstruction driven in part by increased airway smooth muscle responses to contractile stimuli in a process known as airway hyperresponsiveness (AHR) (2–4). Current therapeutic approaches used to treat asthma involve combinatorial administration of bronchodilators and anticholinergic drugs to relax constricted airways and corticosteroids to inhibit airway inflammation (5). Although these treatments benefit many patients who have asthmatic disease, there is a substantial proportion of patients in whom these treatments never fully control asthma, particularly in those who have severe disease (3). Furthermore, cessation of these treatments often results in loss of asthma control and reoccurrence of asthma symptoms, suggesting that these treatments fail to reverse the underlying intrinsic changes in airway cells that mediate asthma pathology (6, 7). Therefore, there is an urgent unmet need for therapeutics that can offer better control and potentially mediate resolution of the disease.

Airway inflammation in allergic asthma is typically driven by type 2 immune responses in the lung, although other asthma endo-types driven by type 2–independent immune responses do exist (8, 9). Type 2 inflammation in the lung is mediated by T helper 2 (T_H2) $CD4^+$ T cells and group 2 innate lymphoid cells (ILC2), which produce the type 2 cytokines, interleukin-4 (IL-4), IL-5, and IL-13, in response to antigen-dependent and antigen-independent activation (10–17). The production and release of these cytokines promote a variety of downstream responses, which include the recruitment and activation of eosinophils in the lung, immunoglobulin E (IgE) production by allergen-specific B cells to arm basophils and mast cells for degranulation, goblet cell–mediated mucus production, and excessive airway smooth muscle contraction, that ultimately result in the damage of the lung parenchyma and the impairment of lung function in asthma (2, 4, 13–16, 18–20). Furthermore, type 2 airway inflammation drives the nonimmune abnormalities, such as AHR, that are present in asthma.

Given the role of T_H2 $CD4^+$ T cells in asthma pathogenesis, blocking T_H2 differentiation of allergen-specific T cells represents a viable therapeutic strategy for the treatment of asthma. Cytokine [e.g., IL-4, TSLP (thymic stromal lymphopoietin), IL-25, and IL-33] and costimulatory (e.g., CD28, ICOS, OX40) signals are important for driving T_H2 differentiation, but the strength and duration of T cell receptor (TCR) signaling can also contribute to the outcome of $CD4^+$ T cell differentiation. Strong and prolonged TCR-

mediated signals promote T_H1 differentiation, whereas weak and transient signals skew differentiation toward T_H2 (21–31). More specifically, TCR-mediated extracellular signal–regulated kinase (ERK) activation is a key determinant in driving $CD4^+$ T cell differentiation, and strong ERK signals block T_H2 differentiation (28, 29). TCR-mediated ERK activation is largely dependent on diacylglycerol (DAG), which is a secondary lipid messenger that is generated after the cleavage of phosphatidylinositol 4,5-bisphosphate (PIP_2) by phospholipase C (PLC). ERK activation is promoted by DAG-mediated Ras-GRP1 activation, and nuclear factor κB (NF-κB) activation is promoted by DAG-mediated PKC activation (32). DAG activity is inhibited by its phosphorylation into phosphatidic acid by DAG kinase (DGK) enzymes. Among DGK family members, the ζ isoform of DGK plays a predominant role in suppressing DAG-dependent ERK activation (33). Accordingly, T cells lacking DGKζ accumulate DAG and display enhanced ERK activation (34).

The absence of DGKζ enhances the magnitude of antitumor and antiviral immunity (34–37). However, in some instances (e.g., in allergic responses), DGKζ knockout (KO) mast cells fail to degranulate, and DGKζ KO mice are resistant to anaphylaxis (38). Thus, depending on the process, blocking DGKζ could be either immunostimulatory or immunosuppressive (39). Given that ERK activation skews T cell responses away from T_H2 differentiation, we hypothesized that the enhancement of DAG signaling by targeting DGKζ would suppress rather than potentiate the development of allergic asthma. We observed that enhancement of DAG signaling by the loss of DGKζ reduced T_H2 differentiation, and this effect translated to protection from a mouse model of T_H2-mediated allergic asthma. Unexpectedly, we found that the mechanisms by which DGKζ promoted airway inflammation and AHR were separable. Conditional deletion of DGKζ in T cells limited type 2 inflammation in an ERK-dependent manner with no effect on AHR. In contrast, targeted deletion of DGKζ in smooth muscle cells impaired AHR without preventing airway inflammation. Furthermore, we found that pharmacological inhibition of DGK suppressed murine type 2 airway inflammation and AHR and inhibited carbachol-mediated bronchoconstriction of human airway slices. Thus, these data demonstrate that DGKs are previously unrecognized therapeutic targets for asthma and reveal that airway inflammation and AHR are not as interdependent as generally believed.

RESULTS

DGKζ KO mice are protected from OVA-induced allergic airway inflammation and AHR

ERK activation drives T cells to differentiate into T_H1 over T_H2 phenotype (28, 29). Because ERK is hyperactivated in the absence of DGKζ in T cells, we tested whether loss of DGKζ in T cells impaired T_H2 differentiation in vitro. When naïve $CD4^+$ T cells from DGKζ KO mice were stimulated through their TCR and expanded in vitro under nonpolarizing conditions, we found that the proportion of T_H1 cells was increased and the proportion of T_H2 cells was decreased when compared with naïve $CD4^+$ T cells from wild-type (WT) mice (Fig. 1, A to C). Because DGKζ KO T cells are hyperproliferative after TCR activation, it was possible that the decrease in the proportion of T_H2 cells was due to selective outgrowth of T_H1 cells among DGKζ KO T cells. However, the total number of T_H2 cells generated after TCR activation in the absence of DGKζ significantly diminished

when compared with WT T cells (fig. S1). In addition, the differentiation of DGKζ KO T cells into T_H2 cells was reduced, whereas T_H1 differentiation was increased at early time points after TCR activation. Thus, these data demonstrate that the loss of DGKζ does not change the kinetics but rather the outcome of T_H differentiation (fig. S2).

Conventional $CD4^+$ T cells can be an early source of IL-4 immediately after TCR activation that is sufficient to promote T_H2 differentiation in the absence of exogenous cytokines (40–42). The generation of T_H2 cells under nonpolarizing conditions was dependent on endogenous production of IL-4 from T cells (fig. S3A). To determine whether reduced T_H2 differentiation in the DGKζ KO T cells was due to impaired endogenous IL-4 production, naïve DGKζ KO $CD4^+$ T cells were activated through their TCR in the presence of exogenous IL-4. We found that T_H2 differentiation was completely restored in DGKζ KO T cells treated with exogenous IL-4 (fig. S3B). Similarly, activation under T_H2-polarizing conditions also restored T_H2 differentiation in DGKζ KO $CD4^+$ T cells (fig. S3C). These data revealed that the addition of exogenous IL-4 during TCR activation could bypass the impairment in T_H2 differentiation in DGKζ KO T cells, which indicated that the loss of DGKζ might impair early TCR-mediated, T cell–intrinsic IL-4 production.

To test whether this reduction in T_H2 differentiation correlated with protection against asthma in DGKζ KO mice, WT and DGKζ KO mice were subjected to an ovalbumin (OVA)–induced allergic asthma mouse model. In line with our in vitro data, total inflammatory cell and eosinophil numbers in the bronchoalveolar lavage (BAL) fluid, the amount of T_H2 cytokines in BAL, and OVA-specific IgG1 serum antibody were significantly reduced in OVA-challenged DGKζ KO mice compared with OVA-challenged WT controls (Fig. 1, D to F). This correlated with decreased inflammatory infiltrates in the lungs of OVA-challenged DGKζ KO mice (Fig. 1G). AHR was almost completely abolished in OVA-challenged DGKζ KO compared with WT mice (Fig. 1H). In contrast to our in vitro data, T_H1 responses were not increased in OVA-challenged DGKζ KO mice, which had no difference in the amount of BAL interferon-γ (IFN-γ) or OVA-specific IgG2a serum antibody compared with WT controls (Fig. 1, E and F). To test whether the loss of DGKζ could protect from other models of allergic asthma, WT and DGKζ KO mice were subjected to chronic house dust mite (HDM) exposure. Airway eosinophilia and the amounts of T_H2 cytokines in the BAL were significantly diminished in HDM-challenged DGKζ KO mice compared with HDM-challenged WT controls (Fig. 1, I and J).

Although DGKζ is the predominant isoform that limits DAG-mediated signaling in T cells, another DGK isoform known as DGKα also contributes to this process (33). In DGKα KO T cells, T_H1 differentiation was enhanced and T_H2 differentiation was reduced after TCR stimulation (fig. S4, A and B). In accordance, AHR and airway inflammation were partially but significantly reduced in OVA-induced DGKα KO mice when compared with WT controls (fig. S4, C to F). Thus, the manipulation of DAG signaling by targeting DGK enzymes attenuates OVA-induced allergic asthma.

Protection from OVA-induced airway inflammation and AHR in the absence of DGKζ is independently mediated by separate compartments

The near-complete abolition of AHR in DGKζ KO mice despite a statistically significant but only partial reduction in airway inflammation prompted us to test whether DGKζ deficiency in nonhematopoietic cells also contributed to protection against OVA-induced allergic asthma. The hematopoietic compartment of lethally irradiated WT and DGKζ KO mice was reconstituted with bone marrow (BM) cells from either WT or DGKζ KO mice. Similar to DGKζ KO mice, eosinophilic inflammation, the amount of T_H2 cytokines in the BAL fluid, and AHR responses were reduced in DGKζ KO➔DGKζ KO BM chimeric mice when compared with WT➔WT BM chimeric mice (Fig. 2, A to C). Unexpectedly, however, we found that the reduction in inflammation and AHR was mediated by two separate cell compartments. Although WT mice reconstituted with DGKζ KO BM cells had reduced eosinophilic inflammation and less T_H2 cytokines in the BAL fluid, they were not protected against OVA-induced AHR (Fig. 2, A to C). In contrast, DGKζ KO mice reconstituted with WT BM cells were completely protected from OVA-induced AHR, despite the presence of eosinophilic inflammation and T_H2 cytokines in the BAL fluid (Fig. 2, A to C). These data suggested that DGKζ deficiency in hematopoietic cells contributes to reduced airway inflammation, whereas loss of DGKζ in nonhematopoietic cells leads to protection against AHR.

DGKζ deficiency in T cells protects from OVA-induced airway eosinophilia and partially attenuates OVA-induced T_H2 differentiation

To more precisely interrogate the impact of DGKζ deficiency in hematopoietic cells in OVA-induced airway inflammation, DGKζ was conditionally deleted in hematopoietic cells or T cells using a Vav-inducible Cre (Vav-Cre DGKζ$^{fl/fl}$ mice) or CD4-inducible Cre (CD4-Cre DGKζ$^{fl/fl}$ mice), respectively. In Vav-Cre DGKζ$^{fl/fl}$ mice OVA-induced eosinophil accumulation and the amount of IL-4 in the BAL fluid were significantly reduced, whereas the OVA-induced AHR response was completely intact (Fig. 2, D to F). Similarly, in CD4-Cre DGKζ$^{fl/fl}$ mice, OVA-induced eosinophil accumulation and the amount of IL-4 in the BAL fluid were also reduced (Fig. 2, G and H).

Whereas IL-4 abundance in the BAL was diminished in Vav-Cre DGKζ$^{fl/fl}$ and CD4-Cre DGKζ$^{fl/fl}$ mice after OVA challenge, the IL-5 and IL-13 amounts in the BAL were relatively intact in these mice (Fig. 2, F and H). To test whether the loss of DGKζ in T cells selectively attenuated the ability of T cells to produce IL-4 after T_H2 differentiation in vivo, we adoptively transferred a mixture of CD45.1$^+$CD45.2$^+$ WT and CD45.2$^+$ DGKζ KO OT-II CD4$^+$ T cells into naïve CD45.1$^+$ WT mice followed by OVA immunization. OT-II T cells express a transgenic TCR specific for the $OVA_{323–339}$ peptide presented on the MHC (major histocompatibility complex) class II I-A^b molecule. In accordance with the Vav-Cre DGKζ$^{fl/fl}$ and CD4-Cre DGKζ$^{fl/fl}$ data, we found that the proportion of DGKζ KO OT-II T cells expressing IL-4 was significantly diminished, whereas the proportions of DGKζ KO OT-II T cells expressing IL-5 and IL-13 were relatively unaltered compared with WT OT-II T cells after OVA sensitization (Fig. 2I and fig. S5). These data suggest that the loss of DGKζ selectively impaired the ability of T cells to produce IL-4 in a T cell–intrinsic manner during T_H2 differentiation in vivo. In addition, we observed that the frequency of DGKζ KO

OT-II T cells expressing IFN-γ was significantly increased compared with WT OT-II T cells after OVA sensitization, suggesting that T_H1 differentiation was enhanced in the absence of DGKζ in vivo (Fig. 2I and fig. S5). Overall, these data demonstrate that DGKζ deficiency inhibits airway inflammation in a T cell–intrinsic manner by partially attenuating T_H2 differentiation in vivo.

DGKζ deficiency in airway smooth muscle cells protects from OVA-induced AHR

AHR is increased indirectly in part by the production of contractile mediators from sensory neurons that innervate the lungs, and directly by contraction of airway smooth muscle cells driven by the activation of receptors, such as muscarinic type 3 (M3) receptors, that bind to these mediators (43–45). Furthermore, DGKζ is expressed in sensory neurons arising from the dorsal root ganglion and in smooth muscle cells (46–50). To identify the nonhematopoietic cell type that was responsible for protection against OVA-induced AHR in the absence of DGKζ, DGKζ was conditionally deleted in sensory neurons (Pirt-Cre DGKζ$^{fl/fl}$) and smooth muscle cells (Myh11-Cre DGKζ$^{fl/fl}$). Pirt-Cre DGKζ$^{fl/fl}$ mice exhibited similar OVA-induced AHR compared with control mice (Fig. 3A). However, Myh11-Cre DGKζ$^{fl/fl}$ mice were protected from OVA-induced AHR despite unaltered airway inflammation (Fig. 3, B to D). Moreover, methacholine-induced contractile force was reduced in tracheal rings isolated from either DGKζ KO or Myh11-Cre DGKζ$^{fl/fl}$ mice when compared with WT or Myh11-Cre controls (Fig. 3, E and F, and fig. S6). These data demonstrate that DGKζ promotes airway smooth muscle cell contraction and allergen-induced AHR independently of inflammation in a cell-intrinsic manner.

Enhancement of ERK signaling in T cells is sufficient to protect from OVA-induced allergic airway inflammation but insufficient to protect from OVA-induced AHR

We tested whether increased ERK signaling was responsible for the effect of DGKζ deficiency on T_H2 differentiation. To this end, we assessed T_H differentiation of naïve DGKζ KO $CD4^+$ T cells activated through their TCR in the presence of the U0126, a pharmacological inhibitor of mitogen-activated protein kinase kinase 1/2 (MEK1/2), the kinase that phosphorylates and activates ERK. We found that inhibition of ERK signaling was sufficient to restore T_H2 differentiation in DGKζ KO T cells (Fig. 4A and fig. S7). In addition, although treatment with U0126 did not alter the frequency of IL-4– and IL-13–producing WT T cells, inhibition of ERK signaling increased the frequency of WT T cells producing IL-5 (Fig. 4A and fig. S7). In contrast, T_H1 differentiation in WT and DGKζ KO T cells was reduced in the presence of U0126. Together, these data establish that enhanced TCR-mediated DAG signaling impairs T_H2 differentiation and promotes T_H1 differentiation in an ERK-dependent manner (Fig. 4A and fig. S7).

We took a gain-of-function approach to test whether the enhancement of ERK signaling in T cells was sufficient to limit OVA-induced airway inflammation. Sevenmaker (ERK^{SEM}) transgenic mice express a transgene that encodes a gain-of-function mutant of Erk2 driven from the human CD2 promoter and locus control region, which results in selective enhancement of the ERK signaling pathway specifically in T cells (51). Similar to DGKζ KO T cells, T_H1 differentiation was increased and T_H2 differentiation was reduced after TCR stimulation of ERK^{SEM} T cells in vitro (Fig. 4, B to D). Furthermore, ERK^{SEM} mice

had less eosinophilia and T_H2 cytokines in the airways after OVA challenge compared with WT controls. Thus, enhancement of ERK signaling was sufficient to inhibit T_H2 differentiation and protect from OVA-induced airway inflammation in vivo (Fig. 4, E and F). Similar to the Vav-Cre DGKζ$^{fl/fl}$ mice, OVA-induced AHR in ERK^{SEM} mice was similar to WT controls, despite suppressed type 2 airway inflammation (Fig. 4G). Overall, these data demonstrate that DGKζ controls T_H2 differentiation in an ERK-dependent manner in T cells to promote OVA-induced airway inflammation independently of AHR.

Pharmacological inhibition of DGK is sufficient to protect from OVA-induced asthma

We tested whether DGK could represent a previously unrecognized target for the prevention and treatment of asthma. Although there are no selective inhibitors of DGKζ, a pan-DGK inhibitor, R59949, that is relatively selective for DGKα is commercially available (52, 53). DGKα and DGKζ are expressed in both T cells and smooth muscle cells (33, 34, 48). Because DGKα KO mice have a partial but statistically significant reduction in OVA-induced airway inflammation and AHR, we tested whether pharmacological inhibition of DGKα kinase activity with R59949 could block OVA-induced type 2 airway inflammation and AHR. Mice were treated with R59949 during the late sensitization and airway challenge phases of the murine model of OVA-induced asthma. Compared with vehicle, treatment with R59949 significantly inhibited AHR and reduced eosinophilia and T_H2 cytokines in the BAL fluid (Fig. 5, A to C). To test whether DGKα inhibition could block type 2 airway inflammation and AHR after allergen-specific T cell responses were established, we treated OVA-sensitized mice with R59949 only during the airway challenge phase of the OVA-induced asthma model. Compared with vehicle, treatment with R59949 again exhibited significantly reduced OVA-induced AHR (Fig. 5D). In contrast, treatment with R59949 during the airway challenge phase failed to alter type 2 airway inflammation after OVA challenge (Fig. 5, E and F). Together, these data suggest that DGK can be pharmacologically targeted to reduce AHR and airway inflammation. However, whereas the acute administration of a DGK inhibitor is sufficient to attenuate OVA-induced AHR, the DGK inhibitor must be administered during the sensitization stage to inhibit the type 2 airway inflammation.

To further examine the therapeutic potential of targeting DGK, we tested whether inhibition of DGKα by R59949 affects human airway smooth muscle (HASM) contraction. Human airway smooth muscle cells were pretreated with or without R59949 and stimulated with the nonselective M3 receptor agonist, carbachol. The phosphorylation of myosin light chain (MLC), a critical step in smooth muscle cell contraction, was reduced by R59949 (Fig. 5G). To test whether this effect translated to the attenuated contraction of human airways, precision-cut lung slices (PCLS) were obtained from lung transplant donors and treated with R59949. After overnight incubation with R59949, carbachol-induced bronchoconstriction was significantly decreased (Fig. 5H). Overall, these data highlight that acute inhibition of DGK is sufficient to protect from the development of AHR in human samples. These data suggest that DGK is a potential therapeutic target for the prevention and treatment of asthma.

DISCUSSION

Our findings demonstrated that augmenting DAG signaling by limiting the activity of DGKζ and DGKα reduced disease in a mouse model of allergen-induced asthma. Genetic ablation of DGKζ or DGKα protected from OVA-induced airway inflammation and AHR. Using BM chimeras, we demonstrated that inhibition of AHR was due to the loss of DGKζ in the radioresistant compartment, whereas reduced airway inflammation was due to the loss of DGKζ in the radio-sensitive compartment. Thus, DGKζ limits these processes in separate compartments and independently of each other. Generation of cell type–specific conditional DGKζ KO mice revealed that the protection from OVA-induced airway inflammation was mediated by the loss of DGKζ in T cells, whereas the attenuation of OVA-induced AHR was facilitated by the absence of DGKζ in airway smooth muscle cells. Last, acute loss of DGK activity through pharmacological blockade with a DGKα inhibitor was sufficient to protect mice from allergen-induced asthma, limit allergen-induced AHR in mice with established allergen-induced immune responses, and reduce carbachol-induced bronchoconstriction of human airways. These data suggest that modulating DGK activity could represent a new therapeutic strategy for the treatment of asthma.

Given that DAG promotes signal transduction downstream of activating receptors, one might predict that the inhibition of DGK would always enhance immune responses. Our findings highlight the idea that augmenting DAG-mediated signaling does not necessarily increase activation. In settings of T_H1 and cell-mediated immune responses, increased DAG signaling caused by the loss of DGKζ augments the function of T cells and NK cells (34–37). In contrast, mast cell degranulation during allergic responses is inhibited in the absence of DGKζ (38). Thus, targeting DGKζ is immunomodulatory, i.e., it is immunostimulatory or immunosuppressive depending on the context. Our data presented here reinforce this notion because the loss of DGKζ inhibits T_H2-mediated inflammation.

We demonstrated that the loss of DGKζ diminished T_H2 differentiation in vitro and suppressed eosinophilic inflammation and T_H2 cytokine release in the BAL fluid of asthmatic mice in vivo. Although all major T_H2 cytokines (IL-4, IL-5, and IL-13) were reduced in the BAL of DGKζ KO mice, only IL-4, but not IL-5 or IL-13, was reduced in the airways of Vav-Cre DGKζ$^{fl/fl}$ and CD4-Cre DGKζ$^{fl/fl}$ mice. In accordance, DGKζ KO OT-II cells displayed a selective impairment in their potential to produce IL-4, but not IL-5 or IL-13, compared with cotransferred WT OT-II cells after OVA sensitization in vivo. These results suggest that the loss of DGKζ selectively impairs the ability of T cells to produce IL-4 in a T cell–intrinsic manner during T_H2 differentiation in vivo. This could potentially explain the selective reduction in BAL IL-4 amounts seen in the hematopoietic-specific and T cell–specific DGKζ KO mice after OVA challenge in vivo. It is still unclear why all three T_H2 cytokines were reduced in WT mice reconstituted with DGKζ KO BM cells. The BM reconstitution studies may need to be interpreted with caution given the unknown effects of irradiation, reconstitution efficiency, and increased age of BM-transplanted mice on asthma.

The signaling mechanism by which DGK deficiency protects against asthma is not entirely clear. We started our studies by hypothesizing that DGK deficiency would limit T_H2 differentiation by enhancing ERK phosphorylation. However, the role of ERK in T_H2

differentiation and allergic asthma is controversial. Although ERK activation downstream of strong TCR stimulation negatively correlates with T_H2 differentiation (22, 29), very strong TCR-mediated signaling can also induce T_H2 differentiation (23). Similarly, in ERK1 KO mice, allergic airway inflammation and AHR were decreased due to reduction in T_H2 differentiation (54), yet others report that T_H2 differentiation is intact in ERK1 KO mice (55). In these studies, the defects in OVA-induced allergic asthma in ERK1 KO mice might be secondary to enhanced IL-12 production by ERK1 KO dendritic cells (56), which stimulates a T_H1 response in a T cell–extrinsic manner. T cells expressing a dominant negative Ras transgene (dnRas Tg mice) exhibit reduced T_H2 differentiation in vitro and in vivo (OVA-induced asthma), which further suggests that ERK activation promotes T_H2 differentiation (57, 58). However, TCR-activated dnRas Tg T cells also display impaired IL-4R signaling as demonstrated by decreased pSTAT6, pJak1, pJak3, and pIL-4Rα after IL-4 stimulation (57). As a result, the defect in T_H2 differentiation seen in dnRas Tg T cells might reflect impaired IL-4–mediated T_H2 polarization. As opposed to DGKζ KO T cells, exogenous IL-4 was not sufficient to restore T_H2 differentiation in dnRas Tg T cells.

Our findings demonstrated that partial attenuation of ERK signaling by U0126 restored T_H2 differentiation in DGKζ KO T cells. Furthermore, T cells from ERK^{SEM} mice showed increased T_H1 and decreased T_H2 differentiation in vitro, which correlated with protection from OVA-induced type 2 airway inflammation in vivo. Thus, the effect of DGKζ deficiency on the inhibition of T_H2 differentiation was dependent on increased ERK activation. However, NF-κB activity is also increased in DGKζ KO T cells after TCR activation (59). Although, whether enhancement of NF-κB signaling also contributes to the attenuation of T_H2 differentiation in DGKζ KO T cells remains unclear. The NF-κB p50 subunit is required for GATA3 expression at late time points after TCR activation under T_H2 polarization conditions (60). Yet, the requirement for the NF-κB p50 subunit and other members of the NF-κB family in the instruction of T_H2 differentiation by weak TCR-mediated signaling is unknown.

The mechanism by which DGK affects acetylcholine-induced smooth muscle cell contraction is still unclear. Akin to what we observed with airway smooth muscle cells, inhibition of DGKα activity also reduces vascular smooth muscle contraction through an unknown mechanism (49, 50). Similar to TCR signaling, activation of muscarinic type 3 receptors, which are G protein–coupled receptors (GPCRs) that signal through $G\alpha_q$ proteins, promotes PLC-dependent DAG generation and ERK activation (61, 62). Thus, it is possible that the attenuation of smooth muscle contraction in DGKζ KO airway smooth muscle cells is also ERK dependent. However, ERK signaling promotes rather than suppresses carbachol-induced contraction in ileal smooth muscle cells and α_1-adrenergic receptor–induced contraction, which is another $G\alpha_q$-coupled GPCR, in vascular smooth muscle cells (63, 64). In addition, PLC activation increases intracellular Ca^{2+} necessary for the cross-bridge cycling of actin and myosin to drive smooth muscle contraction, and DAG-dependent PKC activation maintains contraction by preventing activation of an inhibitor of the cross-bridge cycling (65–67). Consequently, one might expect that the lack of DGKζ, which would lead to enhanced DAG-dependent PKC activation after muscarinic type 3 receptor activation, would exacerbate bronchoconstriction. However, the diminution of smooth muscle contraction by the loss of DGKζ suggests that other biological mechanisms are involved. It

is possible that enhanced DAG-mediated PKC activation results in feedback inhibition of PLC activity, which would lead to diminished Ca^{2+} responses and attenuated smooth muscle contraction. This feedback inhibition of PLC activity is seen after a short term treatment with DAG analogs, such as phorbol esters (68, 69). Similarly, DGKζ KO mast cells display impaired FcεRI-mediated degranulation due to impaired PLCγ and Ca^{2+} responses after FcεRI activation (38).

Our study demonstrated that AHR and eosinophilic airway inflammation were separate and distinct processes that mediated the development of asthma independently of each other. In recent clinical trials, although inhibition of type 2 cytokine signaling reduces eosinophilia and decreases the frequency of asthma exacerbations in asthmatic patients, these approaches failed to improve baseline lung function or prevent histamine-induced airway responses (70, 71). Thus, suppressing inflammation is not sufficient to reverse AHR and airway smooth muscle dysfunction in asthma. Our findings formally demonstrated that airway eosinophilic inflammation and AHR can be regulated independently of each other and revealed that DGKζ plays a central role in the induction of these processes during the development of asthma. We envision that therapeutic targeting of DGKζ may prevent or resolve asthma by suppressing both the immune and nonimmune responses that drive the disease.

MATERIALS AND METHODS

Mice

C57BL/6, B6.SJL-*Ptprc*^{a}*Pepc*^{b}/BoyCrCrl (CD45.1^{+}), and C57BL/6-Tg(TcraTcrb)425Cbn/Crl (CD45.2^{+} WT OT-II) mice were purchased from the Jackson laboratory or Charles River Laboratories. Generation of DGKζ KO, DGKζ floxed (DGKζ$^{fl/fl}$), and DGKα KO mice were described previously (33, 59, 72). CD45.1^{+}CD45.2^{+} WT OT-II mice were generated by crossing CD45.2^{+} WT OT-II to CD45.1^{+} WT mice. CD45.2^{+} DGKζ KO mice were crossed to CD45.2^{+} WT OT-II mice to generate CD45.2^{+} DGKζ KO OT-II mice. C57BL/6-*Il4*^{tm1Nnt}/J (IL-4 KO) mice were purchased from the Jackson laboratory. B6.Cg-*Commd10*$^{Tg(Vav1-icre)A2Kio}$/J (Vav-Cre) and Tg(Cd4-cre)1Cwi/BfluJ (CD4-Cre) mice were purchased from the Jackson laboratory and crossed to DGKζ$^{fl/fl}$ mice to generate Vav-Cre DGKζ$^{fl/fl}$ and CD4-Cre DGKζ$^{fl/fl}$ mice, respectively. B6.Cg-Tg(Myh11-cre,-EGFP)2Mik/J (Myh11-Cre) mice were purchased from the Jackson laboratory and crossed to DGKζ$^{fl/fl}$ mice to generate Myh11-Cre DGKζ$^{fl/fl}$ mice. Pirt-Cre mice were crossed to DGKζ$^{fl/fl}$ mice to generate Pirt-Cre DGKζ$^{fl/fl}$ mice (73). Sevenmaker (ERK^{SEM}) mice were provided by L. Samuelson from the National Institutes of Health and were originally developed by S. Hedrick from the University of California, San Diego (51). Unless otherwise specified, all mice were 7 to 12 weeks old at the time of use, were housed in pathogen-free conditions, and were treated in strict compliance with the Institutional Animal Care and Use Committee regulations at the University of Pennsylvania.

Flow cytometry, cell sorting, and data analysis

For flow cytometric analyses, cells were stained with antibodies against cell surface antigens at 4°C for 15 min in phosphate-buffered saline (PBS). LIVE/DEAD Fixable Aqua Dead Cell Stain Kit was used to exclude nonviable cells. Intracellular cytokine staining was performed

with the BD Cytofix/Cytoperm Kit according to the manufacturer's protocol. Flow cytometry was performed with an LSR II or FACSCanto flow cytometer (BD Biosciences). For cell sorting, freshly isolated splenocytes were stained with fluorescein isothiocyanate (FITC)–conjugated anti-CD4 (GK1.5, eBioscience) and anti-FITC magnetic-activated cell sorting (MACS) beads (Miltenyi Biotec) and, subsequently, passed through MACS columns (Miltenyi Biotec) according to the manufacturer's protocol to enrich for $CD4^+$ T cells. MACS-enriched $CD4^+$ T cells were subjected to cell surface staining before cell sorting. FACS (fluorescence-activated cell sorting) was performed with a FACSAria cell sorter (BD Biosciences). Data were analyzed and plotted with FlowJo software (TreeStar). All fluorochrome-conjugated antibodies are listed in table S1.

$CD4^+$ T cell differentiation assays

MACS-enriched $CD4^+$ T cells were sorted for naïve T cells ($CD4^+CD45RB^+CD25^-CD44^{lo}$). Sorted naïve $CD4^+$ T cells were plated (30,000 cells per well) in tissue culture media [MEMα (Invitrogen) with 10% heat-inactivated fetal bovine serum (FBS; Atlanta Biologicals), penicillin (100 U/ml), streptomycin (100 μg/ml), 2 mM L-glutamine, 12.5 mM Hepes (Life Technologies), and 22.9 μM β-mercaptoethanol (Bio-Rad)] and activated with soluble anti-CD3 (10 μg/ml; 145–2C11, BD Pharmingen) and soluble anti-CD28 (3 μg/ml; 37.51, BD Pharmingen) in the presence of irradiated (50 Gy) CD4-depleted splenocytes (150,000 cells per well). In some experiments, sorted naïve $CD4^+$ T cells were activated in the presence of either media alone or exogenous IL-4 (10 ng/ml; Peprotech) before TCR activation. In other experiments, sorted naïve $CD4^+$ T cells were activated under T_H2 conditions [anti–IL-12 (10 μg/ml; C15.6, BioLegend), anti–IFN-γ (10 μg/ml; XMG1.2, BioLegend), IL-4 (10 ng/ml; Peprotech)]. In other experiments, sorted naïve $CD4^+$ T cells were pretreated with either dimethyl sulfoxide (DMSO) or the MEK1/2 inhibitor U0126 (0.4 μM; Cell Signaling Technology) for 30 min before TCR activation. On day 5 after activation, T cells were restimulated with phorbol 12-myristate 13-acetate (PMA; 100 ng/ml; Sigma-Aldrich) and ionomycin (1 μg/ml; Sigma-Aldrich) in the presence of brefeldin A (5 μg/ml; Cell Signaling Technology) for 5 hours. In other experiments, on day 3 or day 4 after activation, T cells were restimulated with PMA and ionomycin in the presence of brefeldin A for 5 hours. After restimulation, activated T cells were washed twice with PBS and prepared for cell surface and intracellular cytokine staining.

OVA-induced allergic asthma model

Mice were sensitized with an intraperitoneal injection of 10 μg of OVA (Sigma-Aldrich) and 2.25 mg of Imject Alum (Thermo Fisher Scientific), which contains aluminum hydroxide and magnesium hydroxide with inactive stabilizers, in 200 μl of PBS on day 0 and day 14. After sensitization, mice were intranasally challenged with 10 μg of OVA in 20 μl of PBS on days 28 to 30. Airway responses to methacholine were measured about 16 hours after the last intranasal challenge. Mice were anesthetized with an intraperitoneal injection of ketamine (87.5 mg/kg; Hospira Inc.) and xylazene (12.5 mg/kg; Akorn Inc.), cannulated through the trachea, and attached to a lung mechanics analyzer (FlexiVent, SCIREQ Inc.). Airway responses were measured after the administration of increasing doses of methacholine through the use of a nebulizer as we previously described (74). Briefly, mice were ventilated with a tidal volume of 8 ml/kg at a rate of 150 breaths/min and a positive

end-expiratory pressure of 3 cm H_2O by using a computerized flexiVent system. Using the low-frequency forced oscillation technique, respiratory mechanical input impedance (*Zrs*) was derived from the displacement of the ventilator's piston and the pressure in its cylinder. By fitting *Zrs* to the constant phase model, the flexiVent software calculated the airway resistance ($cmH_2O.s.ml^{-1}$), which was normalized to body weight. Baseline measurements and responses to aerosolized saline were followed by measurements of responses to increasing doses of aerosolized methacholine (Sigma-Aldrich, St. Louis, MO). Recorded values were averaged for each dose and used to obtain dose-response curves for each mouse.

After measurement of airway mechanics, the lung was flushed three times with 0.7 ml of MACS buffer [PBS with 5% bovine serum albumin (Fisher Bioreagents) and 2 mM EDTA (Invitrogen)] containing complete Mini, EDTA-free protease inhibitor cocktail (Roche) to collect BAL fluid. The BAL fluid was centrifuged at 6797*g* at 4°C for 2 min in a microcentrifuge. BAL supernatant was collected and stored at −80°C before analysis. For measurement of cytokine concentrations in cell-free BAL fluid, mouse-specific IL-4 (BD Biosciences), IL-5 (BioLegend), and IL-13 (eBioscience) ELISA (enzyme-linked immunosorbent assay) kits were used according to the manufacturer's protocol. The remaining BAL cell pellet was treated with erythrocyte lysis buffer (ELB), pelleted, and resuspended in PBS for analysis by cytospin or flow cytometry. For cytospin analysis, BAL cells were spun down onto cytospin slides using a cytocentrifuge. Slides were air dried and stained with Shandon Kwik-Diff (Thermo Fisher Scientific) according to the manufacturer's protocol. Differential BAL cell counts were performed manually with at least 200 total cells counted for each slide as previously described (75–77). For analysis by flow cytometry, BAL cells were stained with antibodies against cell surface markers and identified by the following gating schemes: eosinophils ($Ly6G^-CD11c^-Siglec\ F^+$), neutrophils ($CD11b^+Ly6G^+$), macrophages ($Ly6G^-F4/80^+$), and lymphocytes ($CD3^+$ or $CD19^+$ or $B220^+$). All cells were pregated on $CD45^+$ live cells.

After BAL fluid collection, murine lungs were injected with 10% buffered formalin (Fisher Healthcare) though the trachea, harvested, and incubated in 10% buffered formalin overnight to allow for fixation. Next, lung tissue was dehydrated, paraffin embedded, and sliced into sections. Tissue sections were stained with hematoxylin and eosin (H&E) to determine cellular infiltrates in the lung (78, 79). Inflammation was scored by two blinded investigators on a scale of 0 (no tissue inflammation) to 5 (severe inflammation with involvement of the peribronchial, perivascular, and parenchymal regions).

HDM-induced allergic asthma model

Mice were intranasally challenged with 25 μg of HDM extract (*Dermatophagoides pteronyssinus*, Greer Laboratories) in 20 μl of PBS for 5 days a week for three consecutive weeks (intranasal HDM challenge on days 0 to 4, days 7 to 11, and days 14 to 18). Mice were taken down 16 hours after the last intranasal challenge, and the lung was flushed once with 0.7 ml of MACS buffer [PBS with 5% bovine serum albumin (Fisher Bioreagents) and 2 mM EDTA (Invitrogen)] containing complete Mini, EDTA-free protease inhibitor cocktail (Roche) to collect BAL fluid. The BAL fluid was processed as described earlier to measure immune cell recruitment and cytokine release in the airways.

Adoptive transfer of WT and DGKζ KO OT-II

MACS-enriched $CD4^+$ T cells isolated from spleens and lymph nodes of $CD45.1^+CD45.2^+$ WT OT-II TCR transgenic mice and $CD45.2^+$DGKζ KO OT-II TCR transgenic mice were sorted for naïve T cells ($CD4^+CD45RB^+CD25^-CD44^{lo}$). Sorted naïve $CD45.1^+CD45.2^+$WT OT-II and $CD45.2^+$ DGKζ KO OT-II cells were transferred intravenously into $CD45.1^+$ WT hosts at a 1:1 ratio (400,000 WT OT-II:400,000 DGKζ OT-II). One day after transfer, mice were subjected to OVA sensitization. Five days after the second intraperitoneal OVA/Alum immunization, splenic $CD4^+$ T cells were isolated by MACS enrichment and restimulated with PMA (100 ng/ml; Sigma-Aldrich) and ionomycin (1 μg/ml; Sigma-Aldrich) in the presence of brefeldin A (5 μg/ml; Cell Signaling Technology) for 5 hours. After restimulation, activated $CD4^+$ T cells were washed twice with PBS and prepared for cell surface and intracellular cytokine staining.

Generation of BM chimeric mice

Donor BM cells from $CD45.1^+$ WT or $CD45.2^+$ DGKζ KO donor mice were transferred (3×10^6 to 4×10^6 BM cells) intravenously into lethally irradiated (11 Gy) $CD45.1^+$ WT or $CD45.2^+$ DGKζ KO hosts. Ten weeks after BM transfer, mice were subjected to OVA sensitization and challenge.

Murine tracheal ring contraction

Airway contractility in isolated murine tracheal rings was determined using multiwire myograph (ADInstruments) as described previously (80). Tracheal rings were mounted on the myograph, bathed in Krebs-Henseleit (K-H) buffer (pH 7.4, 37°C, and 95% O_2/5% CO_2), and baseline tension was set at ~2.5 mN. After the rings attained a stable baseline tension, airways were challenged with increasing concentrations of methacholine and the change in tension was recorded. At the end of the last dose of methacholine, the airways were washed with K-H buffer. Data acquisition and analysis were performed using the Chart 7 software.

Airway contraction measurements in human PCLS

Human PCLS preparation and bronchoconstriction experiments were performed as previously described (81). Briefly, healthy whole lungs from nonasthmatic donors were received from the National Disease Research Interchange (Philadelphia, PA). Lungs were inflated with 2% low–melting temperature agarose, sectioned, cored (8-mm diameter), and sliced at a thickness of 350 μm (Precisionary Instruments VF300 Vibratome). Lung slices were rested in Ham's F12 medium in 12-well tissue culture plates at 37°C for 2 days after isolation and washed three times with fresh media to rid airways of agarose on days 1 and 2 during the resting period. Next, slices were incubated overnight (18 hours) with DMSO or DGK inhibitor R59949 (Sigma-Aldrich). After overnight incubation, slices were challenged with increasing doses of carbachol (Sigma-Aldrich), and live video images of the airways were taken after each dose using a microscope (Nikon Eclipse TE2000-U, ×40 magnification) connected to a live video feed (Evolution QEi 32–0074A-130). Suitable airways on slices were chosen on the basis of the following criteria: presence of a full smooth muscle wall, intact beating cilia, and absence of shared muscle walls at airway

branch points to exclude possible counteracting contractile forces. Changes in airway lumenal area were measured using Image-Pro Plus software (version 6.0, Media Cybernetics) as previously described (81). Area under curve was calculated from the dose-response curves generated.

HASM isolation, culture, and immunoblotting

Primary HASM were generated from nondiseased tracheas received from the National Disease Research Interchange (Philadelphia, PA). HASM culture was performed as previously described (82). HASM cells were cultured in Ham's F12 medium supplemented with 10% FBS, penicillin (100 U/ml), streptomycin (0.1 mg/ml), and amphotericin B (2.5 mg/ml) for up to one to five passages before use.

For immunoblotting analysis, HASM cells were grown to confluence in 12-well tissue culture plates. Cells were serum starved for 24 hours before stimulation. Cells were incubated overnight (18 hours) with DMSO or R59949. After overnight incubation, cells were stimulated with 10 μM carbachol for 10 min. After stimulation, cells were fixed with perchloric acid, scraped, pelleted, and lysed in RIPA (radioimmunoprecipitation assay) buffer. Lysates were subjected to SDS–polyacrylamide gel electrophoresis and transferred to nitro-cellulose membranes. Immunoblotting for phosphorylated MLC (pMLC), phospho-Akt (pAkt), and phosphorylated MLC phosphatase (pMYPT1) was performed using tubulin as a loading control. The antibodies used for immunoblotting are listed in table S2.

In vivo systemic administration of DGK inhibitor

For pharmacological inhibition of DGK activity in vivo, mice were intraperitoneally injected once daily with either DMSO or the DGK inhibitor R59949 (10 mg/kg; Sigma-Aldrich) in 50% polyethylene glycol (PEG) 400 (Sigma-Aldrich) solution beginning immediately after the second intraperitoneal OVA/Alum immunization and ending before the last intranasal OVA challenge (late sensitization and challenge phases) or beginning immediately before the first intranasal OVA challenge and ending before the last intranasal OVA challenge (challenge phase only).

Statistical analysis

Statistical analysis of data was performed with the Prism 6 software (GraphPad).

Supplementary Material

Refer to Web version on PubMed Central for supplementary material.

Acknowledgments:

We thank all members of the Kambayashi, Behrens, Koretzky, Su, Oliver, Silverman, Jordan, and Bassiri laboratories for the advice. We thank L. Samuelson (National Institutes of Health) and C. Sommers (National Institutes of Health) for providing us with the sevenmaker mice. We thank M. Li for carefully reviewing the statistical analyses performed in our studies.

Funding: This work was supported by grants from the American Asthma Foundation (to T.K.), Tobacco-Related Disease Research Program (to A.H.), and the National Institutes of Health (F31-HL134325 to B.K.S.;

T32HL007013 and T32ES007059 to C.H.F.; R21AI116121 and R01AI072197 to A.H.; and R01HL107589, R01HL111501, R01AI121250, and R01HL146645 to T.K.)

REFERENCES AND NOTES

1. Barnett SB, Nurmagambetov TA, Costs of asthma in the United States: 2002–2007. J. Allergy Clin. Immunol 127, 145–152 (2011). [PubMed: 21211649]
2. Lambrecht BN, Hammad H, The immunology of asthma. Nat. Immunol 16, 45–56 (2015). [PubMed: 25521684]
3. Fahy JV, Type 2 inflammation in asthma – present in most, absent in many. Nat. Rev. Immunol 15, 57–65 (2015). [PubMed: 25534623]
4. Locksley RM, Asthma and allergic inflammation. Cell 140, 777–783 (2010). [PubMed: 20303868]
5. Pavord ID, Beasley R, Agusti A, Anderson GP, Bel E, Brusselle G, Cullinan P, Custovic A, Ducharme FM, Fahy JV, Frey U, Gibson P, Heaney LG, Holt PG, Humbert M, Lloyd CM, Marks G, Martinez FD, Sly PD, von Mutius E, Wenzel S, Zar HJ, Bush A, After asthma: Redefining airways diseases. Lancet 391, 350–400 (2017). [PubMed: 28911920]
6. Waalkens HJ, Van Essen-Zandvliet EE, Hughes MD, Gerritsen J, Duiverman EJ, Knol K, Kerrebijn KF; Dutch CNSLD Study Group, Cessation of long-term treatment with inhaled corticosteroid (budesonide) in children with asthma results in deterioration. Am. Rev. Respir. Dis 148, 1252–1257 (1993). [PubMed: 8239161]
7. Haahtela T, Järvinen M, Kava T, Kiviranta K, Koskinen S, Lehtonen K, Nikander K, Persson T, Selroos O, Sovijärvi A, Stenius-Aarniala B, Svahn T, Tammivaara R, Laitinen LA, Effects of reducing or discontinuing inhaled budesonide in patients with mild asthma. N. Engl. J. Med 331, 700–705 (1994). [PubMed: 8058076]
8. Woodruff PG, Modrek B, Choy DF, Jia G, Abbas AR, Ellwanger A, Arron JR, Koth LL, Fahy JV, T-helper type 2-driven inflammation defines major subphenotypes of asthma. Am. J. Respir. Crit. Care Med. 180, 388–395 (2009). [PubMed: 19483109]
9. Anderson GP, Endotyping asthma: New insights into key pathogenic mechanisms in a complex, heterogeneous disease. Lancet 372, 1107–1119 (2008). [PubMed: 18805339]
10. Cohn L, Homer RJ, Marinov A, Rankin J, Bottomly K, Induction of airway mucus production by T helper 2 (Th2) cells: A critical role for interleukin 4 in cell recruitment but not mucus production. J. Exp. Med 186, 1737–1747 (1997). [PubMed: 9362533]
11. Cohn L, Tepper JS, Bottomly K, IL-4-independent induction of airway hyperresponsiveness by Th2, but not Th1, cells. J. Immunol 161, 3813–3816 (1998). [PubMed: 9780144]
12. Cohn L, Homer RJ, MacLeod H, Mohrs M, Brombacher F, Bottomly K, Th2-induced airway mucus production is dependent on IL-4Ralpha, but not on eosinophils. J. Immunol 162, 6178–6183 (1999). [PubMed: 10229862]
13. Brusselle GG, Kips JC, Tavernier JH, van der Heyden JG, Cuvelier CA, Pauwels RA, Bluethmann H, Attenuation of allergic airway inflammation in IL-4 deficient mice. Clin. Exp. Allergy 24, 73–80 (1994). [PubMed: 8156448]
14. Corry DB, Folkesson HG, Warnock ML, Erle DJ, Matthay MA, Wiener-Kronish JP, Locksley RM, Interleukin 4, but not interleukin 5 or eosinophils, is required in a murine model of acute airway hyperreactivity. J. Exp. Med 183, 109–117 (1996). [PubMed: 8551213]
15. Wills-Karp M, Luyimbazi J, Xu X, Schofield B, Neben TY, Karp CL, Donaldson DD, Interleukin-13: Central mediator of allergic asthma. Science 282, 2258–2261 (1998). [PubMed: 9856949]
16. Grünig G, Warnock M, Wakil AE, Venkayya R, Brombacher F, Rennick DM, Sheppard D, Mohrs M, Donaldson DD, Locksley RM, Corry DB, Requirement for IL-13 independently of IL-4 in experimental asthma. Science 282, 2261–2263 (1998). [PubMed: 9856950]
17. Licona-Limón P, Kim LK, Palm NW, Flavell RA, TH2, allergy and group 2 innate lymphoid cells. Nat. Immunol 14, 536–542 (2013). [PubMed: 23685824]
18. Coffman RL, Carty J, A T cell activity that enhances polyclonal IgE production and its inhibition by interferon-gamma. J. Immunol 136, 949–954 (1986). [PubMed: 2934482]

19. Coffman RL, Ohara J, Bond MW, Carty J, Zlotnik A, Paul WE, B cell stimulatory factor-1 enhances the IgE response of lipopolysaccharide-activated B cells. J. Immunol 136, 4538–4541 (1986). [PubMed: 3486902]
20. Vitetta ES, Ohara J, Myers CD, Layton JE, Krammer PH, Paul WE, Serological, biochemical, and functional identity of B cell-stimulatory factor 1 and B cell differentiation factor for IgG1. J. Exp. Med 162, 1726–1731 (1985). [PubMed: 3932582]
21. Le Gros G, Ben-Sasson SZ, Seder R, Finkelman FD, Paul WE, Generation of interleukin 4 (IL-4)-producing cells in vivo and in vitro: IL-2 and IL-4 are required for in vitro generation of IL-4-producing cells. J. Exp. Med 172, 921–929 (1990). [PubMed: 2117636]
22. Constant S, Pfeiffer C, Woodard A, Pasqualini T, Bottomly K, Extent of T cell receptor ligation can determine the functional differentiation of naive CD4+ T cells. J. Exp. Med 182, 1591–1596 (1995). [PubMed: 7595230]
23. Hosken NA, Shibuya K, Heath AW, Murphy KM, O'Garra A, The effect of antigen dose on CD4+ T helper cell phenotype development in a T cell receptor-alpha beta-transgenic model. J. Exp. Med 182, 1579–1584 (1995). [PubMed: 7595228]
24. Tao X, Constant S, Jorritsma P, Bottomly K, Strength of TCR signal determinesthe costimulatory requirements for Th1 and Th2 CD4+ T cell differentiation. J. Immunol 159, 5956–5963 (1997). [PubMed: 9550393]
25. Rulifson IC, Sperling AI, Fields PE, Fitch FW, Bluestone JA, CD28 costimulation promotes the production of Th2 cytokines. J. Immunol 158, 658–665 (1997). [PubMed: 8992981]
26. Jember AG-H, Zuberi R, Liu F-T, Croft M, Development of allergic inflammation in a murine model of asthma is dependent on the costimulatory receptor OX40. J. Exp. Med 193, 387–392 (2001). [PubMed: 11157058]
27. Gonzalo JA, Tian J, Delaney T, Corcoran J, Rottman JB, Lora J, Al-garawi A, Kroczek R, Gutierrez-Ramos JC, Coyle AJ, ICOS is critical for T helper cell–mediated lung mucosal inflammatory responses. Nat. Immunol 2, 597–604 (2001). [PubMed: 11429543]
28. Jorritsma PJ, Brogdon JL, Bottomly K, Role of TCR-induced extracellular signal-regulated kinase activation in the regulation of early IL-4 expression in naive $CD4^+$ T cells. J. Immunol 170, 2427–2434 (2003). [PubMed: 12594266]
29. Yamane H, Zhu J, Paul WE, Independent roles for IL-2 and GATA-3 in stimulating naive $CD4^+$ T cells to generate a Th2-inducing cytokine environment. J. Exp. Med 202, 793–804 (2005). [PubMed: 16172258]
30. Van Dyken SJ, Nussbaum JC, Lee J, Molofsky AB, Liang HE, Pollack JL, Gate RE, Haliburton GE, Ye CJ, Marson A, Erle DJ, Locksley RM, A tissue checkpoint regulates type 2 immunity. Nat. Immunol 17, 1381–1387 (2016). [PubMed: 27749840]
31. Rochman Y, Dienger-Stambaugh K, Richgels PK, Lewkowich IP, Kartashov AV, Barski A, Khurana Hershey GK, Leonard WJ, Singh H, TSLP signaling in $CD4^+$ T cells programs a pathogenic T helper 2 cell state. Sci. Signaling 11, eaam8858 (2018).
32. Ebinu JO et al., RasGRP, a Ras guanyl nucleotide-releasing protein with calcium- and diacylglycerol-binding motifs. Science 280, 1082–1086 (1998). [PubMed: 9582122]
33. Joshi RP, Schmidt AM, Das J, Pytel D, Riese MJ, Lester M, Diehl JA, Behrens EM, Kambayashi T, Koretzky GA, The ζ isoform of diacylglycerol kinase plays a predominant role in regulatory T cell development and TCR-mediated ras signaling. Sci. Signal 6, ra102 (2013). [PubMed: 24280043]
34. Zhong X-P, Hainey EA, Olenchock BA, Jordan MS, Maltzman JS, Nichols KE, Shen H, Koretzky GA, Enhanced T cell responses due to diacylglycerol kinase ζ deficiency. Nat. Immunol 4, 882–890 (2003). [PubMed: 12883552]
35. Riese MJ, Grewal J, Das J, Zou T, Patil V, Chakraborty AK, Koretzky GA, Decreased diacylglycerol metabolism enhances ERK activation and augments $CD8^+$ T cell functional responses. J. Biol. Chem 286, 5254–5265 (2011). [PubMed: 21138839]
36. Riese MJ, Wang L-CS, Moon EK, Joshi RP, Ranganathan A, June CH, Koretzky GA, Albelda SM, Enhanced effector responses in activated $CD8^+$ T cells deficient in diacylglycerol kinases. Cancer Res. 73, 3566–3577 (2013). [PubMed: 23576561]
37. Yang E, Singh BK, Paustian AM, Kambayashi T, Diacylglycerol kinase ζ is a target to enhance NK cell function. J. Immunol 197, 934–941 (2016). [PubMed: 27342844]

38. Olenchock BA, Guo R, Silverman MA, Wu JN, Carpenter JH, Koretzky GA, Zhong X-P, Impaired degranulation but enhanced cytokine production after Fc epsilonRI stimulation of diacylglycerol kinase ζ -deficient mast cells. J. Exp. Med 203, 1471–1480 (2006). [PubMed: 16717114]
39. Singh BK, Kambayashi T, The immunomodulatory functions of diacylglycerol kinase ζ. Front. Cell Dev. Biol 4, 96 (2016). [PubMed: 27656643]
40. Noben-Trauth N, Hu-Li J, Paul WE, Conventional, naive $CD4^+$ T cells provide an initial source of IL-4 during Th2 differentiation. J. Immunol 165, 3620–3625 (2000). [PubMed: 11034364]
41. Liu Z, Liu Q, Hamed H, Anthony RM, Foster A, Finkelman FD, Urban JF Jr., Gause WC, IL-2 and autocrine IL-4 drive the in vivo development of antigen-specific Th2 T cells elicited by nematode parasites. J. Immunol 174, 2242–2249 (2005). [PubMed: 15699158]
42. Croft M, Swain SL, Recently activated naive CD4 T cells can help resting B cells, and can produce sufficient autocrine IL-4 to drive differentiation to secretion of T helper 2-type cytokines. J. Immunol 154, 4269–4282 (1995). [PubMed: 7536767]
43. Erle DJ, Sheppard D, The cell biology of asthma. J. Cell Biol. 205, 621–631 (2014). [PubMed: 24914235]
44. Tränkner D, Hahne N, Sugino K, Hoon MA, Zuker C, Population of sensory neurons essential for asthmatic hyperreactivity of inflamed airways. Proc. Natl. Acad. Sci. U.S.A. 111, 11515–11520 (2014). [PubMed: 25049382]
45. Bergner A, Sanderson MJ, Acetylcholine-induced calcium signaling and contraction of airway smooth muscle cells in lung slices. J. Gen. Physiol 119, 187–198 (2002). [PubMed: 11815668]
46. Ding L, McIntyre TM, Zimmerman GA, Prescott SM, The cloning and developmental regulation of murine diacylglycerol kinase ζ. FEBS Lett. 429, 109–114 (1998). [PubMed: 9657393]
47. Sasaki H, Hozumi Y, Hasegawa H, Ito T, Takagi M, Ogino T, Watanabe M, Goto K, Gene expression and localization of diacylglycerol kinase isozymes in the rat spinal cordand dorsal root ganglia. Cell Tissue Res. 326, 35–42 (2006). [PubMed: 16758180]
48. Nakano T, Hozumi Y, Goto K, Wakabayashi I, Localization of diacylglycerol kinase ε on stress fibers in vascular smooth muscle cells. Cell Tissue Res. 337, 167–175 (2009). [PubMed: 19421779]
49. Nobe K, Miyatake M, Nobe H, Sakai Y, Takashima J, Momose K, Novel diacylglycerol kinase inhibitor selectively suppressed an U46619-induced enhancement of mouse portal vein contraction under high glucose conditions. Br. J. Pharmacol 143, 166–178 (2004). [PubMed: 15289283]
50. Choi H, Allahdadi KJ, Tostes RCA, Webb RC, Diacylglycerol kinase inhibition and vascular function. Curr. Enzyme Inhib. 5, 148–152 (2009).
51. Sharp LL, Schwarz DA, Bott CM, Marshall CJ, Hedrick SM, The influence of the MAPK pathway on T cell lineage commitment. Immunity 7, 609–618 (1997). [PubMed: 9390685]
52. Sato M, Liu K, Sasaki S, Kunii N, Sakai H, Mizuno H, Saga H, Sakane F, Evaluations of the selectivities of the diacylglycerol kinase inhibitors R59022 and R59949 among diacylglycerol kinase isozymes using a new non-radioactive assay method. Pharmacology 92, 99–107 (2013). [PubMed: 23949095]
53. Arranz-Nicolás J, Ogando J, Soutar D, Arcos-Pérez R, Meraviglia-Crivelli D, Mañes S, Mérida I, Ávila-Flores A, Diacylglycerol kinase α inactivation is an integral component of the costimulatory pathway that amplifies TCR signals. Cancer Immunol. Immunother 67, 965–980 (2018). [PubMed: 29572701]
54. Goplen N, Karim Z, Guo L, Zhuang Y, Huang H, Gorska MM, Gelfand E, Pagés G, Pouysségur J, Alam R, ERK1 is important for Th2 differentiation and development of experimental asthma. FASEB J. 26, 1934–1945 (2012). [PubMed: 22262639]
55. Chang C-OF, D'Souza WN, Ch'en IL, Pages G, Pouyssegur J, Hedrick SM, Polar opposites: Erk direction of CD4 T cell subsets. J. Immunol 189, 721–731 (2012). [PubMed: 22675204]
56. Agrawal A, Dillon S, Denning TL, Pulendran B, ERK1−/− mice exhibit Th1 cell polarization and increased susceptibility to experimental autoimmune encephalomyelitis. J. Immunol 176, 5788–5796 (2006). [PubMed: 16670284]
57. Yamashita M, Kimura M, Kubo M, Shimizu C, Tada T, Perlmutter RM, Nakayama T, T cell antigen receptor-mediated activation of the Ras/mitogen-activated protein kinase pathway controls

interleukin 4 receptor function and type-2 helper T cell differentiation. Proc. Natl. Acad. Sci. U.S.A. 96, 1024–1029 (1999). [PubMed: 9927687]

58. Shibata Y, Kamata T, Kimura M, Yamashita M, Wang C-R, Murata K, Miyazaki M, Taniguchi M, Watanabe N, Nakayama T, Ras activation in T cells determines the development of antigen-induced airway hyperresponsiveness and eosinophilic inflammation. J. Immunol 169, 2134–2140 (2002). [PubMed: 12165542]
59. Schmidt AM, Zou T, Joshi RP, Leichner TM, Pimentel MA, Sommers CL, Kambayashi T, Diacylglycerol kinase ζ limits the generation of natural regulatory T cells. Sci. Signal 6, ra101 (2013). [PubMed: 24280042]
60. Das J, Chen CH, Yang L, Cohn L, Ray P, Ray A, A critical role for NF-κB in Gata3 expression and T_H2 differentiation in allergic airway inflammation. Nat. Immunol 2, 45–50 (2001). [PubMed: 11135577]
61. Caulfield MP, Muscarinic receptors—Characterization, coupling and function. Pharmacol. Ther 58, 319–379 (1993). [PubMed: 7504306]
62. Kim HR, Hoque M, Hai C-M, Cholinergic receptor-mediated differential cytoskeletal recruitment of actin- and integrin-binding proteins in intact airway smooth muscle. Am. J. Physiol. Cell Physiol. 287, C1375–C1383 (2004). [PubMed: 15269004]
63. Dessy C, Kim I, Sougnez CL, Laporte R, Morgan KG, A role for MAP kinase in differentiated smooth muscle contraction evoked by α-adrenoceptor stimulation. Am. J. Physiol 275, C1081–C1086 (1998). [PubMed: 9755061]
64. Ihara E, Yu Q, Chappellaz M, MacDonald JA, ERK and p38MAPK pathways regulate myosin light chain phosphatase and contribute to Ca^{2+} sensitization of intestinal smooth muscle contraction. Neurogastroenterol. Motil 27, 135–146 (2015). [PubMed: 25557225]
65. Taylor DA, Stull JT, Calcium dependence of myosin light chain phosphorylation in smooth muscle cells. J. Biol. Chem 263, 14456–14462 (1988). [PubMed: 3170551]
66. Somlyo AP, Somlyo AV, Ca^{2+} sensitivity of smooth muscle and nonmuscle myosin II: Modulated by G proteins, kinases, and myosin phosphatase. Physiol. Rev 83, 1325–1358 (2003). [PubMed: 14506307]
67. Kitazawa T, Eto M, Woodsome TP, Khalequzzaman M, Phosphorylation of the myosin phosphatase targeting subunit and CPI-17 during Ca^{2+} sensitization in rabbit smooth muscle. J. Physiol 546, 879–889 (2003). [PubMed: 12563012]
68. Ryu SH, Kim U-H, Wahl MI, Brown AB, Carpentern G, Huang K-P, Rhee SG, Feedback regulation of phospholipase C-β by protein kinase C. J. Biol. Chem 265, 17941–17945 (1990). [PubMed: 2211670]
69. Ozawa K, Yamada K, Kazanietz MG, Blumberg PM, Beaven MA, Different isozymes of protein kinase C mediate feedback inhibition of phospholipase C and stimulatory signals for exocytosis in rat RBL-2H3 cells. J. Biol. Chem 268, 2280–2283 (1993). [PubMed: 8381401]
70. Noonan M, Korenblat P, Mosesova S, Scheerens H, Arron JR, Zheng Y, Putnam WS, Parsey MV, Bohen SP, Matthews JG, Dose-ranging study of lebrikizumab in asthmatic patients not receiving inhaled steroids. J. Allergy Clin. Immunol 132, 567–574.e512 (2013). [PubMed: 23726041]
71. Liu Y, Zhang S, Li DW, Jiang SJ, Efficacy of anti-interleukin-5 therapy with mepolizumab in patients with asthma: A meta-analysis of randomized placebo-controlled trials. PLOS ONE 8, e59872 (2013). [PubMed: 23544105]
72. Liu C-H, Machado FS, Guo R, Nichols KE, Burks AW, Aliberti JC, Zhong X-P, Diacylglycerol kinase ζ regulates microbial recognition and host resistance to *Toxoplasma gondii*. J. Exp. Med 204, 781–792 (2007). [PubMed: 17371930]
73. Anderson M, Zheng Q, Dong X, Investigation of pain mechanisms by calcium imaging approaches. Neurosci. Bull 34, 194–199 (2018). [PubMed: 28501905]
74. Yang Q, Ge MQ, Kokalari B, Redai IG, Wang X, Kemeny DM, Bhandoola A, Haczku AF, Group 2 innate lymphoid cells mediate ozone-induced airway inflammation and hyperresponsiveness in mice. J. Allergy Clin. Immunol 137, 571–578 (2016). [PubMed: 26282284]
75. Sharma SK, Almeida FA, Kierstein S, Hortobagyi L, Lin T, Larkin A, Peterson J, Yagita H, Zangrilli JG, Haczku A, Systemic FasL neutralization increases eosinophilic inflammation in a mouse model of asthma. Allergy 67, 328–335 (2012). [PubMed: 22175699]

76. Kierstein S, Krytska K, Sharma S, Amrani Y, Salmon M, Panettieri RA, Zangrilli J, Haczku A, Ozone inhalation induces exacerbation of eosinophilic airway inflammation and hyperresponsiveness in allergen-sensitized mice. Allergy 63, 438–446 (2008). [PubMed: 18315731]

77. Kierstein S, Poulain FR, Cao Y, Grous M, Mathias R, Kierstein G, Beers MF, Salmon M, Panettieri RA, Haczku A, Susceptibility to ozone-induced airway inflammation is associated with decreased levels of surfactant protein D. Respir. Res 7, 85 (2006). [PubMed: 16740162]

78. Haczku A, Atochina EN, Tomer Y, Cao Y, Campbell C, Scanlon ST, Russo SJ, Enhorning G, Beers MF, The late asthmatic response is linked with increased surface tension and reduced surfactant protein B in mice. Am. J. Physiol. Lung Cell. Mol. Physiol 283, L755–L765 (2002). [PubMed: 12225952]

79. Jiang Z, Fehrenbach ML, Ravaioli G, Kokalari B, Redai IG, Sheardown SA, Wilson S, Macphee C, Haczku A, The effect of lipoprotein-associated phospholipase A_2 deficiency on pulmonary allergic responses in *Aspergillus fumigatus* sensitized mice. Respir. Res 13, 100 (2012). [PubMed: 23140447]

80. Deshpande DA, Theriot BS, Penn RB, Walker JK, β-Arrestins specifically constrain β2-adrenergic receptor signaling and function in airway smooth muscle. FASEB J. 22, 2134–2141 (2008). [PubMed: 18337459]

81. Cooper PR, Panettieri RA, Steroids completely reverse albuterol-induced β_2-adrenergic receptor tolerance in human small airways. J. Allergy Clin. Immunol 122, 734–740 (2008). [PubMed: 18774166]

82. Panettieri RA, Murray RK, DePalo LR, Yadvish PA, Kotlikoff MI, A human airway smooth muscle cell line that retains physiological responsiveness. Am. J. Physiol 256, C329–C335 (1989). [PubMed: 2645779]

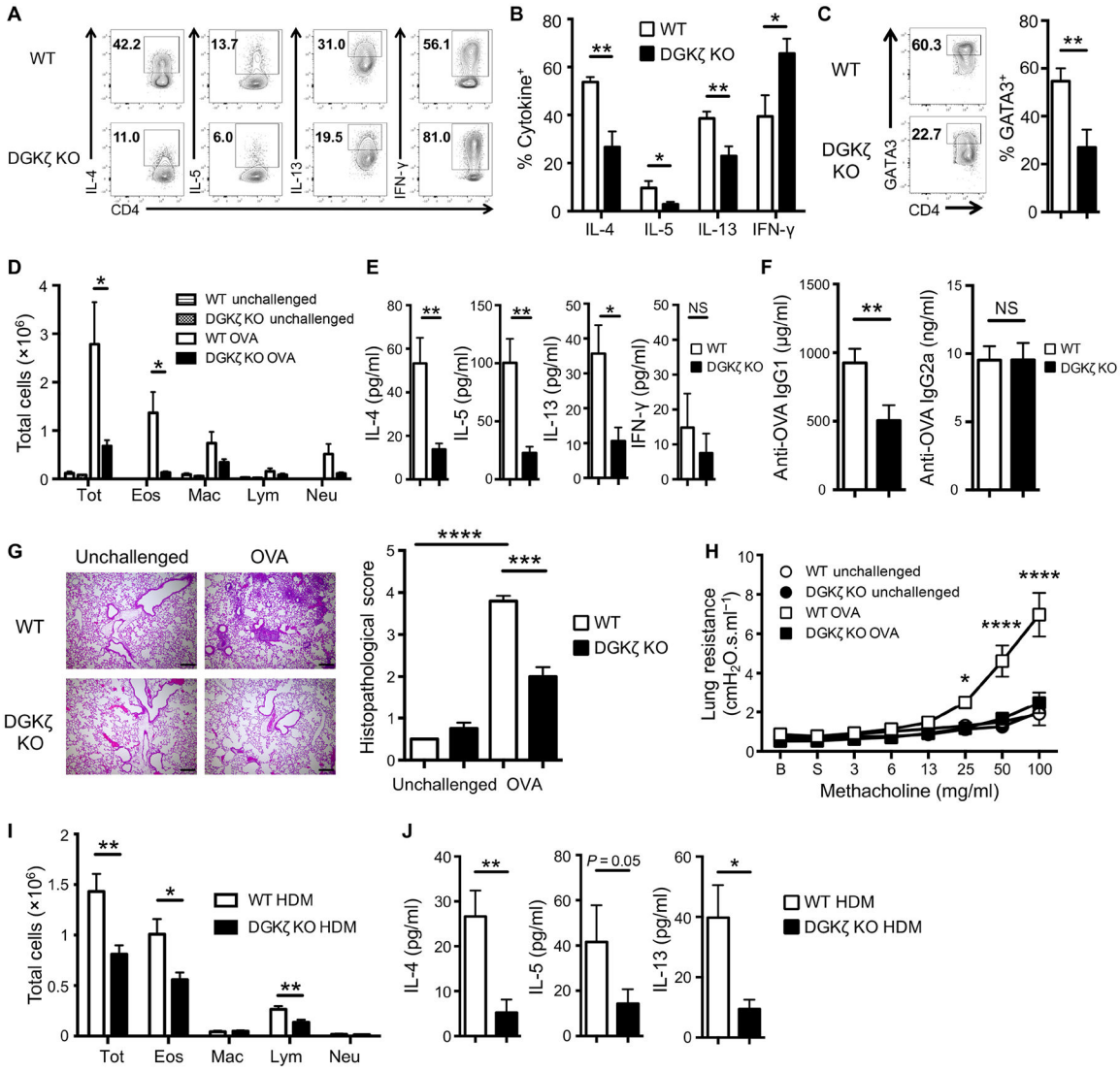

Fig. 1. DGKζ KO mice are protected from OVA-induced allergic airway inflammation and AHR.

(**A** to **C**) Flow cytometry analysis of cytokine production and GATA3 abundance in WT and DGKζ KO $CD4^+$ T cells activated in vitro with antibodies against CD3 and CD28 for 5 days. Dot plots (A and C) are representative of five independent experiments. The frequency of cytokine-producing cells (B) and the frequency of $GATA3^+$ cells (C) are means ± SEM of 10 mice per group pooled from all experiments. (**D**) Cytospin analysis of total number of eosinophils (Eos), macrophages (Mac), lymphocytes (Lym), and neutrophils (Neu) in BAL fluid from unchallenged or OVA-challenged WT and DGKζ KO mice, as indicated. Data are means ± SEM of 6 mice per group (unchallenged) and 19 to 22 mice per group (OVA-challenged) from three independent experiments. (**E** and **F**) ELISA analysis of the amount of T_H1 and T_H2 cytokines in BAL fluid (E) and OVA-specific IgG1 and IgG2a antibody in the serum (F) from OVA-challenged WT and DGKζ KO mice. Data are means ± SEM of 14 to 16 mice per group from two independent experiments. (**G**) H&E staining of lung tissue (left) and compiled histopathological scores (right) from unchallenged and OVA-challenged WT and DGKζ KO mice. Images (left) are representative of two independent experiments. Scale

bars, 200 μm. Quantified scores (right) are means ± SEM of four to five mice per group pooled from all experiments. (**H**) FlexiVent analysis of airway resistance after methacholine treatment of unchallenged or OVA-challenged WT and DGKζ KO mice, as indicated. Data are means ± SEM of six to nine mice per group from two independent experiments. (**I** and **J**) Flow cytometry analysis of total immune cells (I) and ELISA for cytokine amounts (J) in BAL fluid from HDM-challenged WT and DGKζ KO mice. Data are means ± SEM of nine mice per group from two independent experiments. *$P < 0.05$, **$P < 0.01$, ***$P < 0.001$, ****$P < 0.0001$; NS, not significant by two-sided unpaired Student's *t* test (B to G and I), two-way analysis of variance (ANOVA) with Bonferroni's posttest (H), or Mann-Whitney *U* test (J).

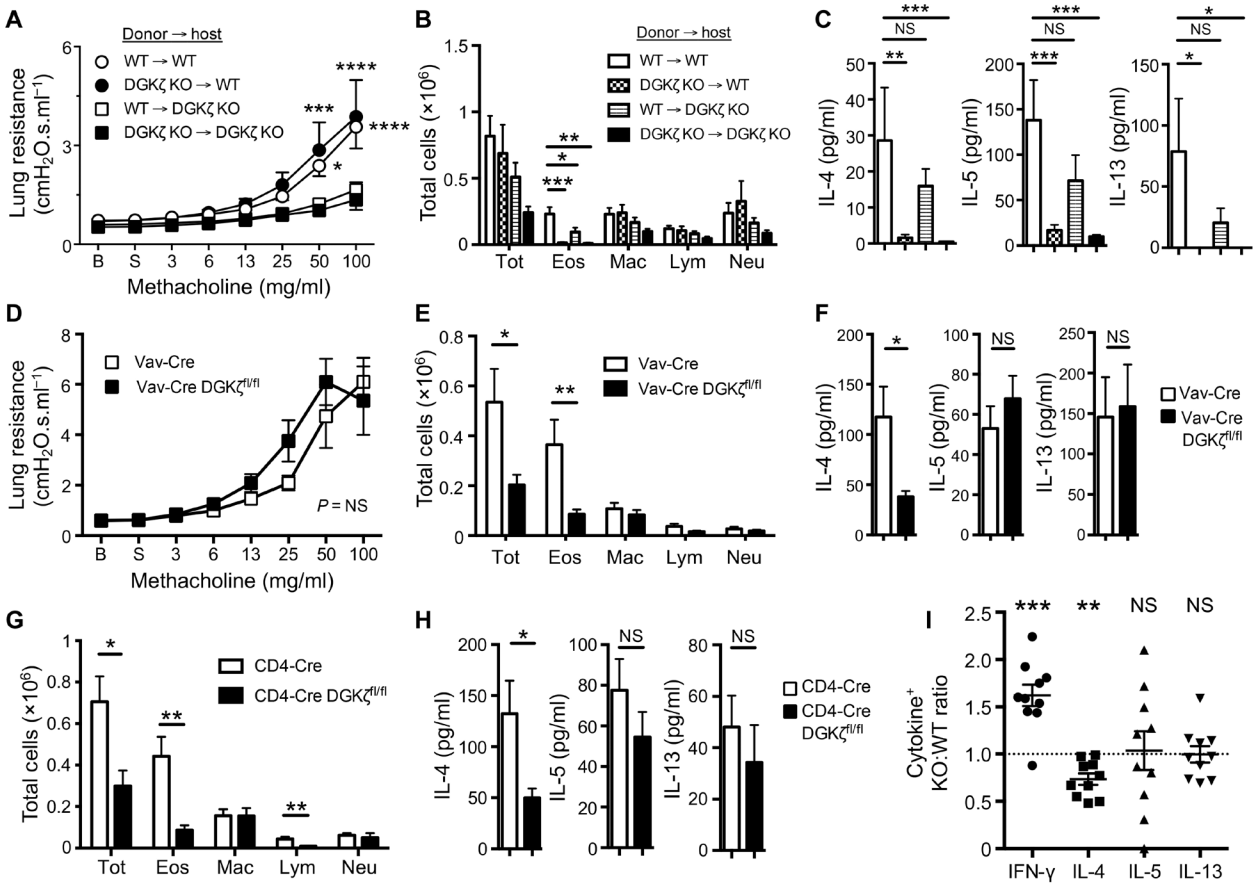

Fig. 2. Hematopoietic and nonhematopoietic cells differentially contribute to OVA-induced airway inflammation and AHR in the absence of DGKζ.

(**A** to **C**) FlexiVent analysis of airway resistance after methacholine treatment (A), cytospin analysis of total immune cells in BAL fluid (B), and ELISA for cytokine abundance in BAL fluid (C) from OVA-challenged WT and DGKζ KO BM chimeras. Data are means ± SEM of seven to nine mice per group from three independent experiments. (**D** to **F**) FlexiVent analysis of airway resistance after methacholine treatment (D), cytospin analysis of total immune cells in BAL fluid (E), and ELISA for cytokine abundance in BAL fluid (F) from OVA-challenged Vav-Cre DGKζ$^{fl/fl}$ mice and Vav-Cre controls. Lung resistance values (D) are means ± SEM of seven mice per group from two independent experiments. BAL cell numbers (E) and cytokine abundance (F) are means ± SEM of 13 to 14 mice per group from four independent experiments. (**G** and **H**) Cytospin analysis of total immune cells (G) and ELISA for cytokine amounts (H) in BAL fluid from OVA-challenged CD4-Cre DGKζ$^{fl/fl}$ mice and CD4-Cre controls. Data are means ± SEM of 12 to 17 mice per group from at least two independent experiments. (**I**) Flow cytometry analysis of the ratio of adoptively transferred cytokine-producing WT OT-II and DGKζ KO OT-II CD4$^+$ T cells in the spleen of OVA-sensitized congenic WT hosts after ex vivo restimulation with PMA/ionomycin. Data are means ± SEM of 10 mice per group from two independent experiments. *$P < 0.05$, **$P < 0.01$, ***$P < 0.001$, ****$P < 0.0001$; NS, not significant by two-way ANOVA with Bonferroni's posttest (A and D), two-sided unpaired Student's *t* test (B and E to H), Mann-Whitney *U* test (C), or one-sided Student's *t* test (I).

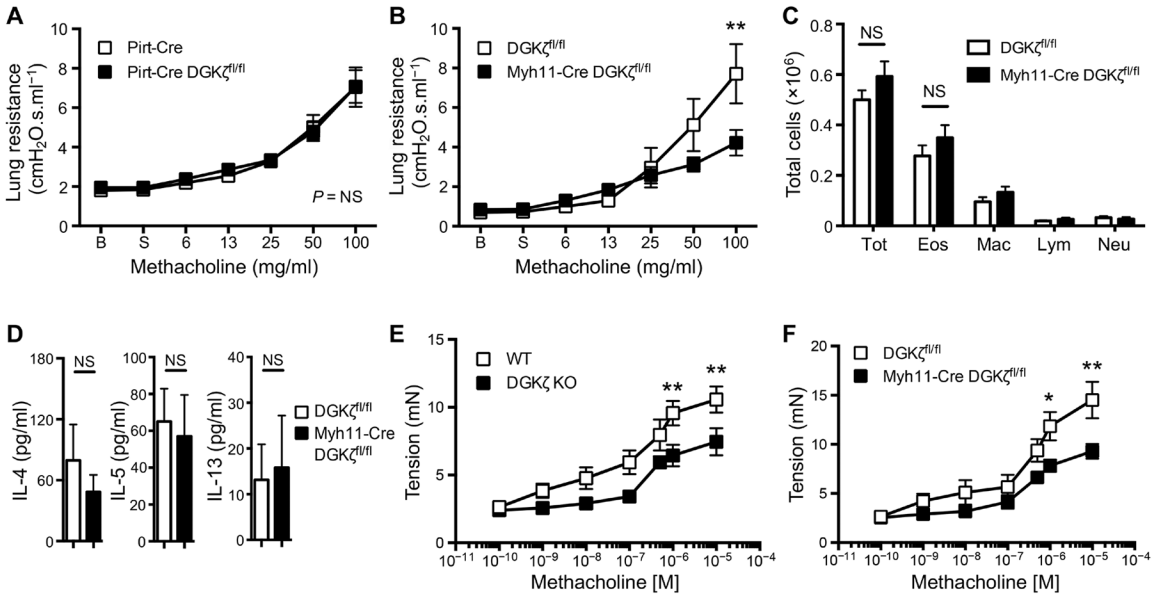

Fig. 3. The loss of DGKζ in airway smooth muscle cells protects against AHR.

(**A**) FlexiVent analysis of airway resistance after methacholine treatment from OVA-challenged Pirt-Cre controls and Pirt-Cre DGKζ$^{fl/fl}$ mice. Data are means ± SEM of 8 to 11 mice per group from two independent experiments. (**B** to **D**) FlexiVent analysis of airway resistance after methacholine treatment (A), flow cytometry analysis of total immune cells in BAL fluid (B), and ELISA for cytokine abundance in BAL fluid (C) from OVA-challenged DGK$^{fl/fl}$ controls and Myh11-Cre DGKζ$^{fl/fl}$ mice. Lung resistance values (B) are means ± SEM of 9 to 14 mice per group from four independent experiments. BAL cell numbers (C) and cytokine abundance (D) are means ± SEM of 18 to 21 mice per group from six independent experiments. (**E**) Myograph analysis of the contractile forces generated after methacholine treatment ex vivo of tracheal rings isolated from WT and DGKζ KO mice. Data are means ± SEM of 8 to 11 mice per group from three independent experiments. (**F**) Myograph analysis of the contractile forces generated after methacholine treatment ex vivo of tracheal rings isolated from DGK$^{fl/fl}$ controls and Myh11-Cre DGKζ$^{fl/fl}$ mice. Data are means ± SEM of eight mice per group from two independent experiments. *$P < 0.05$, **$P < 0.01$; NS, not significant by two-way ANOVA with Bonferroni's posttest (A, B, E, and F) or two-sided unpaired Student's *t* test (C and D).

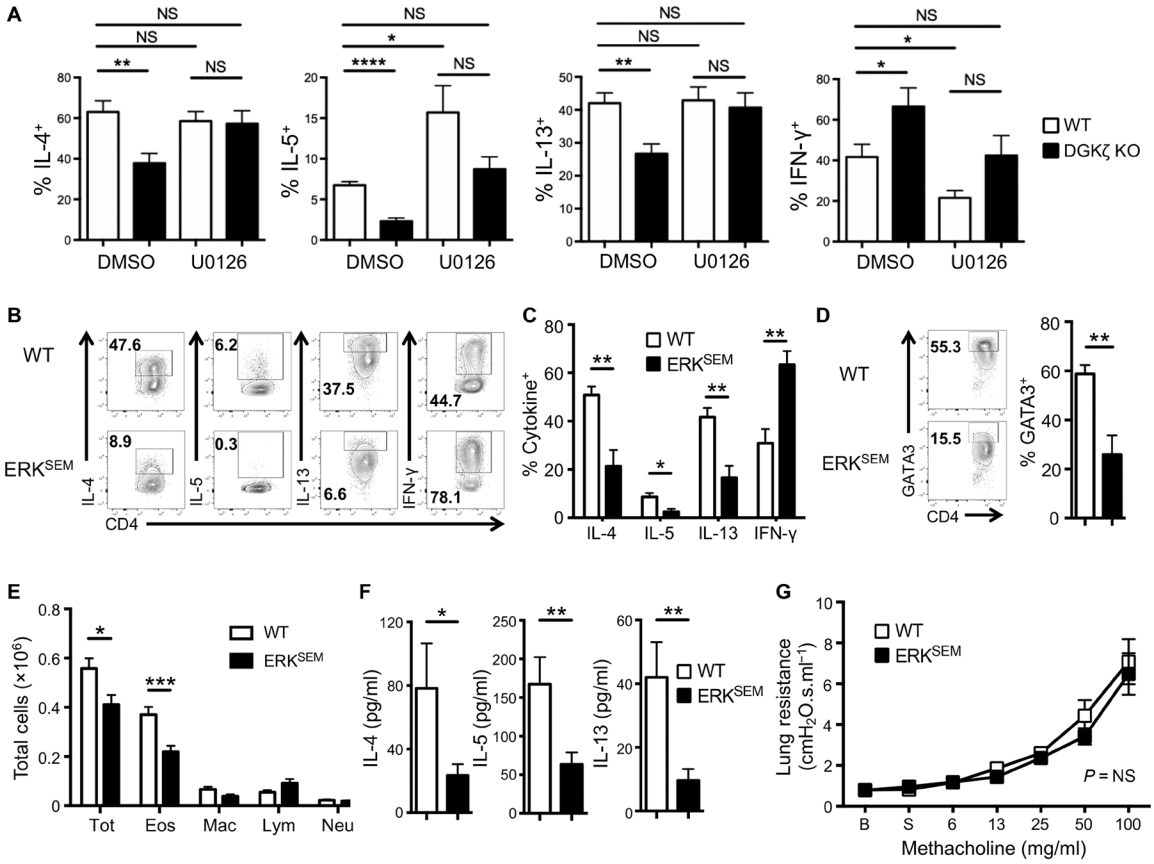

Fig. 4. Enhancement of ERK signaling in T cells is sufficient to protect from OVA-induced allergic airway inflammation but insufficient to protect from OVA-induced AHR.

(**A**) The frequency of cytokine-producing WT and DGKζ KO $CD4^+$ T cells after pretreatment with either vehicle control or U0126 followed by in vitro activation with antibodies against CD3 and CD28 for 5 days. Data are means ± SEM of five mice per group from two independent experiments. (**B** to **D**) Flow cytometry analysis of cytokine production and GATA3 abundance in WT and ERK^{SEM} $CD4^+$ T cells after in vitro activation with antibodies against CD3 and CD28 for 5 days. Dot plots (B and D) are representative of three independent experiments. The frequency of cytokine-producing cells (C) and the frequency of GATA3-expressing cells (D) are means ± SEM of six mice per group from three independent experiments. (**E** to **G**) Flow cytometry analysis of total immune cells in BAL fluid (E), ELISA for cytokine abundance in BAL fluid (F), and flexiVent analysis of airway resistance after methacholine treatment (G) from OVA-challenged WT and ERK^{SEM} mice. BAL cell numbers (E) and cytokine abundance (F) are means ± SEM of 21 to 26 mice per group from five independent experiments. Lung resistance values (G) are means ± SEM of eight to nine mice per group from two independent experiments. $*P < 0.05$, $**P < 0.01$, $***P < 0.001$, $****P < 0.0001$; NS, not significant by two-sided unpaired Student's *t* test (A to F) or two-way ANOVA with Bonferroni's posttest (G).

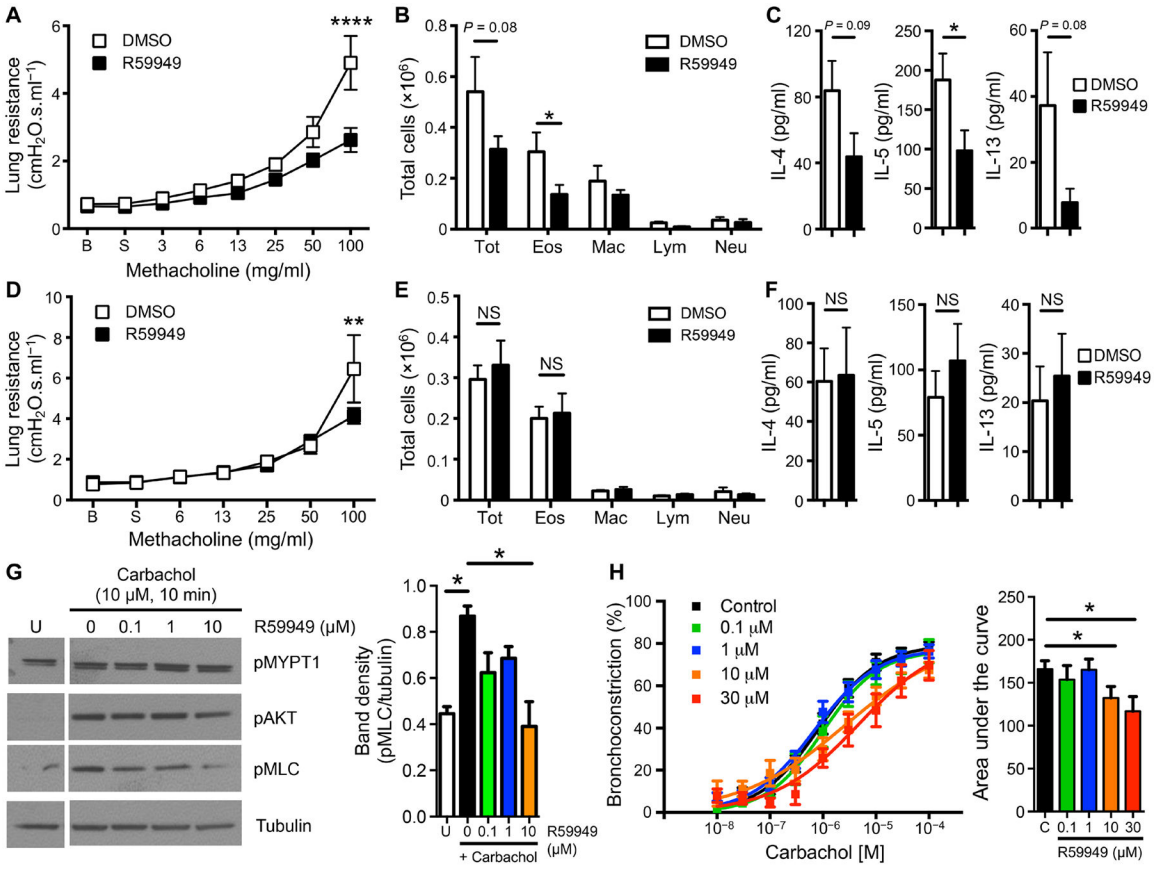

Fig. 5. Pharmacological inhibition of DGK protects against OVA-induced allergic airway inflammation and AHR.

(**A** to **C**) FlexiVent analysis of airway resistance after methacholine treatment (A), flow cytometry analysis of total immune cells in BAL fluid (B), and ELISA for cytokine abundance in BAL fluid (C) from OVA-challenged WT mice treated with either vehicle control or R59949 during the late sensitization and airway challenge phases of the OVA-induced asthma model. Lung resistance values (A) are means ± SEM of seven to eight mice per group from three independent experiments. BAL cell numbers (B) are means ± SEM of 15 to 17 mice per group from four independent experiments. Cytokine amounts (C) are means ± SEM of 10 to 11 mice per group from two independent experiments. (**D** to **F**) FlexiVent analysis of airway resistance after methacholine treatment (D), flow cytometry analysis of total immune cells in BAL fluid (E), and ELISA for cytokine abundance in BAL fluid (F) from OVA-challenged WT mice treated with either vehicle control or R59949 only during the airway challenge phase of the OVA-induced asthma model. Data are means ± SEM of 9 to 10 mice per group from two independent experiments. (**G**) Western blot for pMLC, pAkt, and pMYPT1 in lysates of carbachol-stimulated HASM cells pretreated with vehicle versus R59949. Blots (left) are representative of three independent experiments. Normalized band densities of pMLC (right) are means ± SEM of three donors per condition pooled from all experiments. (**H**) Analysis of bronchoconstriction (left) and area under curve values (right) after carbachol treatment of human PCLS pretreated with vehicle versus R59949. Data are means ± SEM of 9 to 23 slices per condition from three to seven donors

per condition. *$P < 0.05$, **$P < 0.01$, ****$P < 0.0001$; NS, not significant by two-way ANOVA with Bonferroni's posttest (A and D) or two-sided unpaired Student's *t* test (B, C, and E to H).